SRYAHWA PUBLICATIONS

Annals of Archaeology
ISSN: 2639-3662 | Volume 8, Issue 2, 2026
https://doi.org/10.22259/2639-3662.0802004

RESEARCH ARTICLE

New Insights on Metallurgical and Ceremonial Activity During the Iron Age II in SAR53, Saruq Al-Hadid (Dubai, UAE)

Eric Vilanova[1], Fernando Contreras[1], Esther Fernández[1], Dr Mansour Boraik[2], Dr Anjana Reddy[2]

[1]*Sanisera Archaeology Institute, Ciutadella de Menorca, Balearic Islands, Spain.*
[2]*Dubai Culture and Arts Authority, Dubai, United Arab Emirates.*

Received: 09 July 2026 Accepted: 26 July 2026 Published: 30 July 2026

Corresponding Author: Eric Vilanova, Sanisera Archaeology Institute, Ciutadella de Menorca, Balearic Islands, Spain.

Abstract

The 2025 excavation of the SAR53 site within Saruq al-Hadid (Dubai, UAE), conducted by the Sanisera Archaeology Institute under the supervision of the Dubai Culture and Arts Authority, examined two areas of the site (Areas O and T) and identified activity dating to the Iron Age II. The principal phase, dated to the 9th–early 8th century BCE, combined copper production and the deliberate deposition of ritual objects within the same sector, where metalworking residues were recovered alongside snake figurines, serpent-decorated pottery, weaponry, and other symbolically charged items such as soft-stone vessels, jewellery, and shells bearing pigment. A later phase is associated with charcoal production linked to the supply of fuel for metallurgical processes. Previously interpreted as a peripheral fuel-supply zone for the neighbouring SAR7 sector, SAR53 instead emerges as a self-contained locus of the same practices, suggesting that the embedding of metallurgy within ceremonial life was not restricted to SAR7 but formed part of a broader pattern structuring Saruq al-Hadid as a whole.

Keywords: Saruq Al-Hadid, SAR53· Iron Age II, Copper Metallurgy, Ceremonial Activity, Snake Iconography, Charcoal Production, UAE

1. Introduction

1.1 Saruq Al-Hadid: Site and Research History

Saruq al-Hadid is located on the northern fringe of the Rubʿal-Khālī desert, within the Emirate of Dubai, UAE (24°39′55″ N, 55°14′24″ E). Characterised by long-term seasonal occupation spanning from the Neolithic to the early Islamic period, the site has yielded exceptional evidence of Bronze and Iron Age craft production and ritual economy (Weeks et al. 2017; Herrmann, Casana & Qandil 2012; Valente et al. 2022). The artefactual record peaks in intensity during Iron Age II (ca. 1100–600 BCE), when large-scale copper metallurgy — encompassing all stages from smelting to finished object production — transformed the site into a unique industrial centre within the southeastern Arabian landscape (Valente 2023; Weeks et al. 2017). The assemblage is dominated by copper alloy objects, including weapons, tools, vessels, jewellery, and snake figurines, alongside large volumes of smelting slag, copper ingots, and production residues. Snake imagery — in the form of appliqué decoration on ceramic vessels and copper alloy figurines — is a recurrent feature of the Iron Age II assemblages and links the site to a wider southeastern Arabian tradition of serpent symbolism attested at contemporary cultic sites such as Bithnah, Masafi, and Al Qusais (Weeks et al. 2017; Benoist 2007). The co-occurrence of intensive metallurgical activity with deliberately deposited ritual objects has led researchers to interpret Saruq al-Hadid through the theoretical lens of a ritual economy — a place where craft production, social cohesion, and cultic practice were deeply intertwined (Valente 2023; Weeks et al. 2017).

Citation: Eric Vilanova, Fernando Contreras, Esther Fernández, *et al.* New Insights on Metallurgical and Ceremonial Activity During the Iron Age II in SAR53, Saruq Al-Hadid (Dubai, UAE). Annals of Archaeology. 2026;8(2): 54-74.

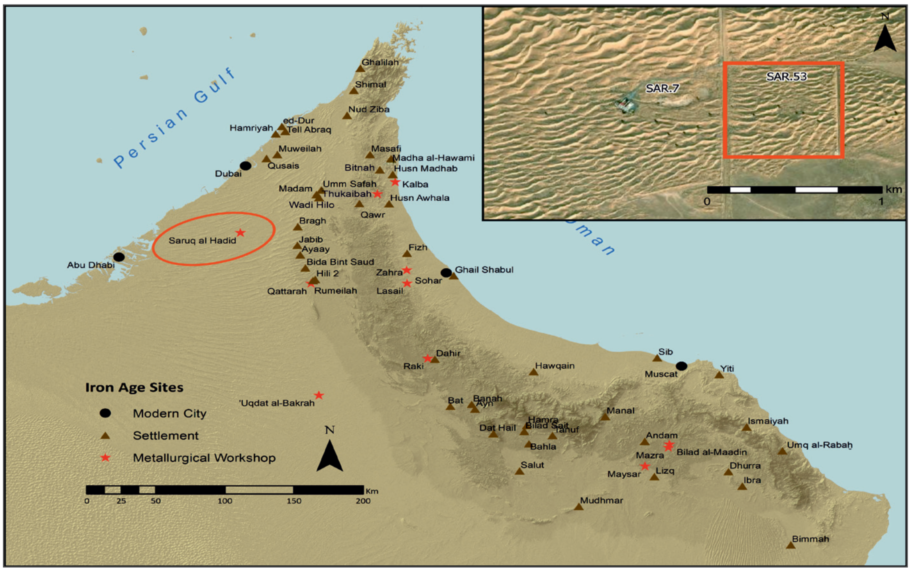

Figure 1. *Overview map of Saruq Al-Hadid and SAR53. Base map and site distribution adapted from Valente (2023) and Al Suwaidi (2025), with modifications by the authors.*

Since its discovery by H.H Sheikh Mohammed in 2002, the site has been the focus of sustained international research, conducted by the Jordanian mission (Al-Khraysheh & An-Nashef 2007), the Dubai Desert Survey (Casana, Herrmann & Qandil 2009), the local team of Dubai Government (DM&DCAA), the SHARP project (Weeks et al. 2017; 2019a), the Polish Mission (Wygnańska et al. 2022), the German Mission (Ihde 2017), and the Sanisera Archaeology Institute, which conducted five seasons of fieldwork in Areas 2A and G between 2015 and 2019 (Contreras et al. 2017; Valente et al. 2020). Most research has concentrated on SAR7, the main excavation locus, defined by dense accumulations of copper slag and metal artefacts with evidenc of smelting, refining, artefact production, and recycling from the Bronze Age through to the early Islamic period (Valente 2020; Weeks et al. 2022).

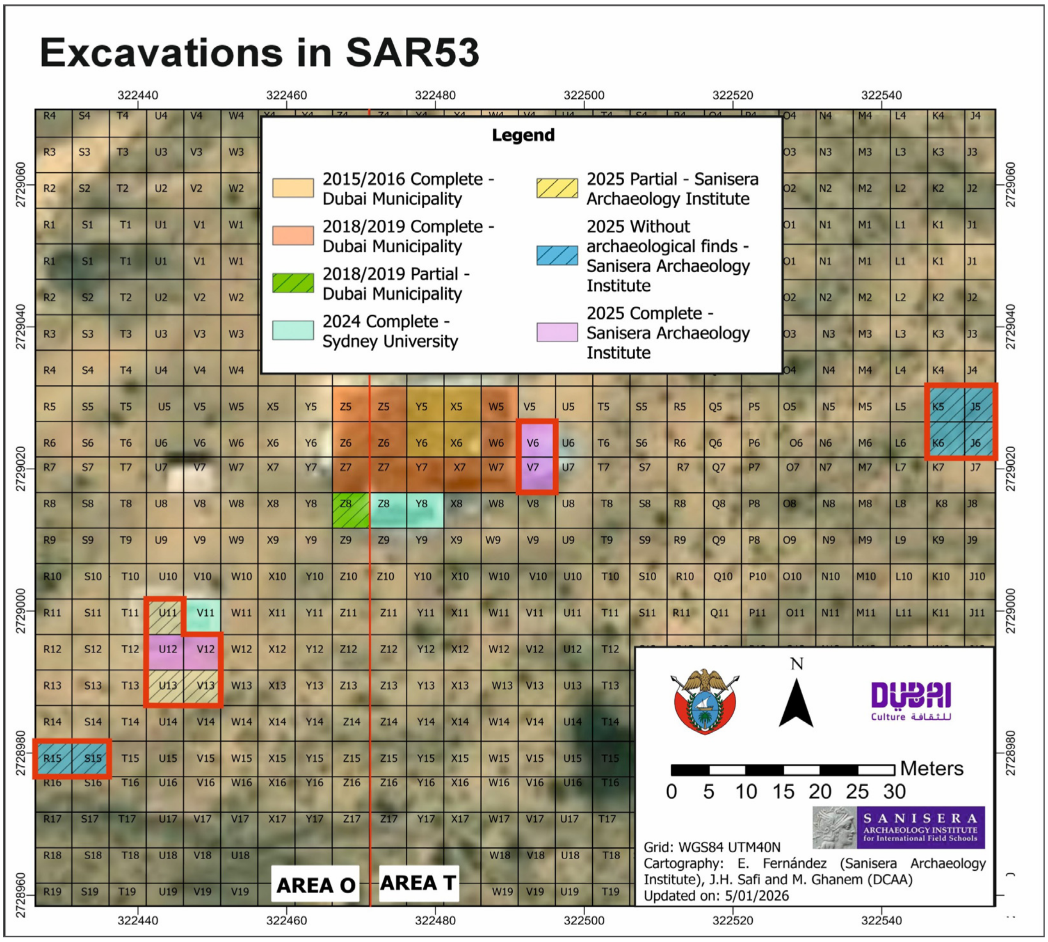

Figure 2. *Squares excavated in SAR53, with the squares excavated during the 2025 Sanisera Archaeology Institute campaign outlined in red.*

1.2 Background of SAR53

The site lies approximately 540 m east of SAR7. It was first documented during the 2007 surveys, which recorded surface concentrations of fire-altered sandstone, charcoal-rich deposits, and Iron Age pottery (Boraik 2020, p. 117). A 10 × 10 m sounding in 2015–2016 reached the gypsum bedrock at c. 3.2 m depth, and the 2018–2019 campaign opened Areas T and O, exposing a sequence of Iron Age II layers of ash, charcoal, and aeolian sand together with numerous pits cut into the bedrock and interpreted as charcoal-production features (Al Suwaidi et al. 2025, pp. 232, 234).

On the basis of these dense charcoal deposits and the absence of metallurgical slag in the excavated record, SAR53 was characterised primarily as a charcoal-production area, tentatively related to the fuel demands of metal smelting elsewhere within Saruq al-Hadid (Boraik 2020, pp. 117, 119, 122) and treated as a possible auxiliary site whose relationship to SAR7 still requires further study (Al Suwaidi et al. 2025, p. 231).

The same 2018–2019 campaign also recovered, within a sealed circular pit (90 cm in diameter) in Layer 2 of Area T, an intentionally deposited hoard of over 100 objects, predominantly copper-alloy vessels and tools, subsequently published in detail by Al Suwaidi et al. (2025, p. 233). Direct evidence for in-situ metalworking came instead from the 2024 University of Sydney season, which recovered slag fragments, primary copper ingot pieces, molten metal droplets, and dross demonstrating that metalworking occurred within SAR53 itself.

1.3 The 2025 Sanisera Session

Prior to excavation, a GIS analysis of GPR data published by Santos-Assunção *et al.* (2025) was carried out in ArcGIS Pro to identify areas of highest archaeological potential within SAR53. Two priority zones were identified and guided the initial placement of excavation squares in Area T (K5, K6, J5, J6) and Area O (R15, S15). Excavation of these squares, combined with targeted test pits reaching the gypsum bedrock, confirmed the absence of significant stratified deposits in both areas. In Area T, aerial photography from 2016 revealed evidence of heavy machinery activity that had reworked the sediments, accounting for the absence of intact archaeological contexts despite the geophysical anomalies. These results informed a revised strategy, developed in coordination with the Dubai Culture and Arts Authority, concentrating fieldwork on squares immediately adjacent to the grids excavated in 2018–2019 and 2024. This decision led to the opening of five squares in Area O (U11, U12, U13, V12, V13) and two in Area T (V6, V7), which produced the stratigraphic and material evidence presented in this paper.

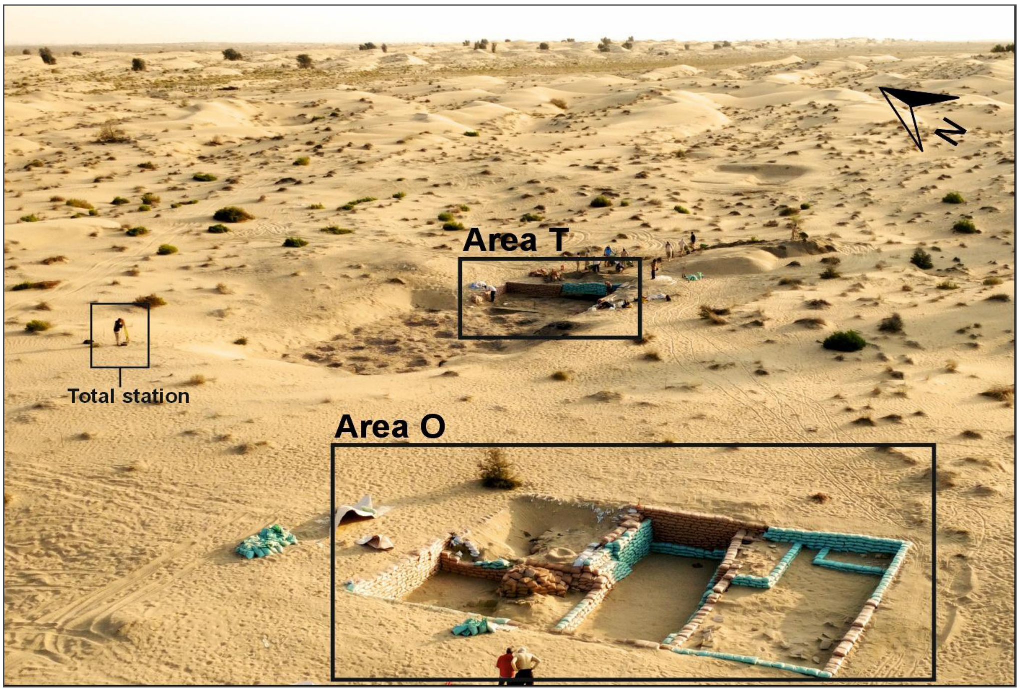

Figure 3. *Aerial view of excavations with archaeological finds in Area T and Area O.*

2. Stratigraphic Sequence and Chronological Framework

2.1 Area O

The stratigraphic sequence in Area O comprises three layers. Layer 1, the uppermost deposit, is a loose aeolian sand without archaeological content. Layer 2, the principal occupation horizon, consists of loose aeolian sand with inclusions of charcoal, sandstone, and abundant archaeological material. The depositional surface was not horizontal but followed the gradient of the underlying natural dune, a slope that accounts for the vertical scatter of finds across the excavated squares. The altimetric variation in find elevations is therefore interpreted as reflecting a single depositional event, or closely successive events within the same occupational phase, rather than distinct stratigraphic sub-phases. This is supported by the ceramic assemblage, in which numerous sherds refit into a small number of original vessels, indicating that the vertically dispersed material derives from a limited set of objects deposited together rather than from successive depositional episodes. Layer 3, the earliest horizon, consists of compacted sand with moderate gypsum content directly overlying the gypsum bedrock. The layer contains a series of small fireplace features concentrated in squares V12 and U12.

2.1.1 Phase 1: Low-Intensity Earlier Occupation (Layer 3)

Layer 3 contains eleven small fireplaces in squares U12 (Contexts 6 and 7) and V12 (Contexts 6–16) (Fig. 4), ranging from simple ashy lenses to more defined circular and oval pit features, including one clustered with surrounding stones (Fig. 4a). The deepest, Context 16 (32 × 49 × 27 cm), penetrates slightly into the gypsum bedrock. In U12, Features 8 and 5 are at slightly lower elevations than the rest, indicating a degree of superimposition consistent with successive episodes of activity. The associated assemblage is sparse and largely undiagnostic: small flint flakes constitute the most recurrent find category (Fig. 4c), accompanied by minor quantities of faunal remains and a few sherds of coarse, undecorated pottery. The complete absence of diagnostic Iron Age II material culture — consistently present in the overlying Layer 2 — confirms the stratigraphic priority of this horizon and its definition as Phase 1. It is characterised by low-intensity, episodic activity most plausibly representing brief, repeated visits to the area before the more structured activities of the Iron Age II.

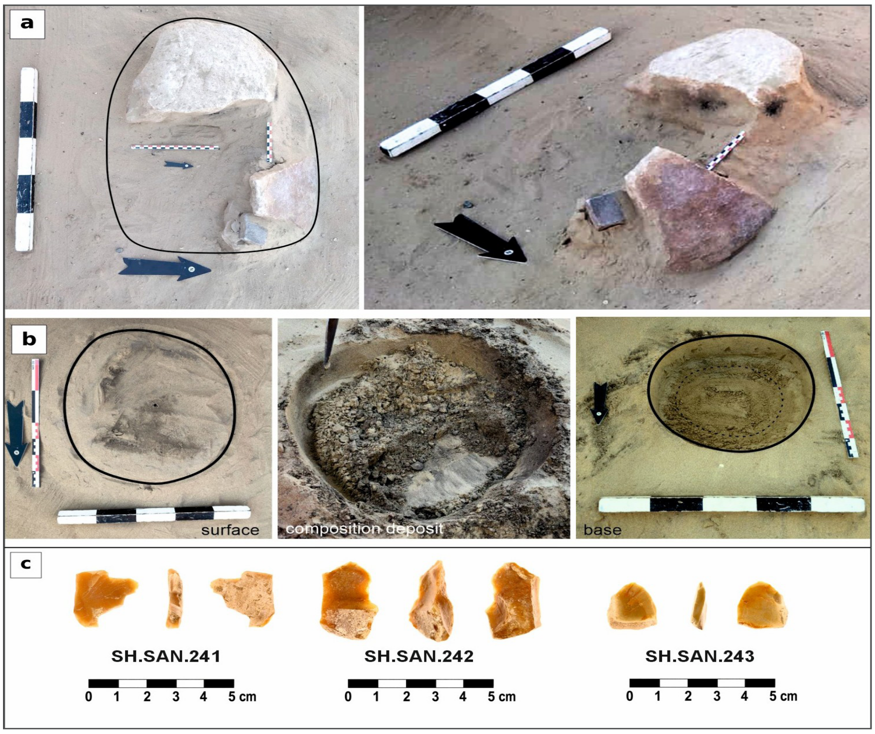

Figure 4. *Phase 1. a) Clustered fireplace within V12. b) Circular fireplace within U12. c) Selection of flint flakes from Layer 3. The assemblage includes unretouched cortical flakes (SH.SAN.241 and SH.SAN.242), and a retouched flake (SH.SAN.243).*

2.1.2 Phase 2: Metallurgical Production and Ritual Deposition (Layer 2)

Layer 2 is the richest and most complex horizon identified in the campaign and, unlike the underlying Layer 3, yields diagnostic Iron Age II material culture, including diagnostic pottery such as snake-decorated sherds and a bridge-spouted vessel**.** Its character is defined by the co-occurrence of metallurgical production evidence and deliberate ritual deposition, whose spatial rlationship is central to the interpretation of the site. Scattered and clustered sandstone blocks are distributed across all five squares (Fig. 5, 6a).

Scattered and clustered sandstone blocks are distributed across all five squares. In U11, structure 3 (Fig. 6b) consists of a tightly arranged cluster of sandstones associated with a thin charcoal-rich lens (c. 3 cm) in the adjacent area; it is only partially exposed owing to the overlying structure 2, which prevents a precise functional assessment, although the associated charcoal lens is consistent with a combustion feature.

Approximately 0.7 m above it, four vertically placed stones form structure 2 of indeterminate function in the south-east of the square (Fig. 6c). In the adjacent square V11, a subcircular, plaster-lined combustion structure was recorded by the University of Sydney (Lehner et al., 2025, unpublished report). In square U13, two linear arrangements of predominantly horizontally placed sandstones (structures 4 and 5) occupy the northern and southern portions of the square respectively.

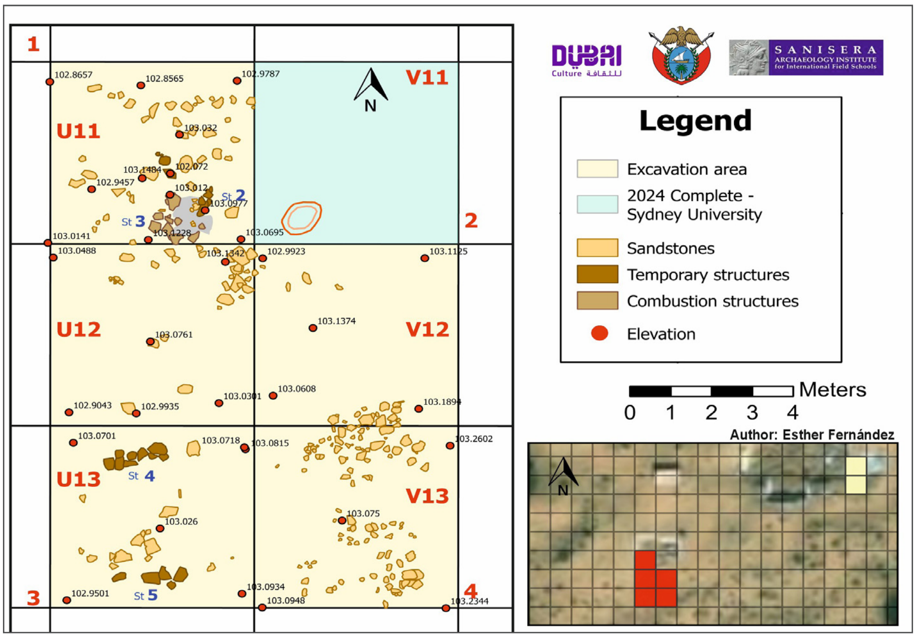

Figure 5. *Plan view of Layer 2 in Area O.*

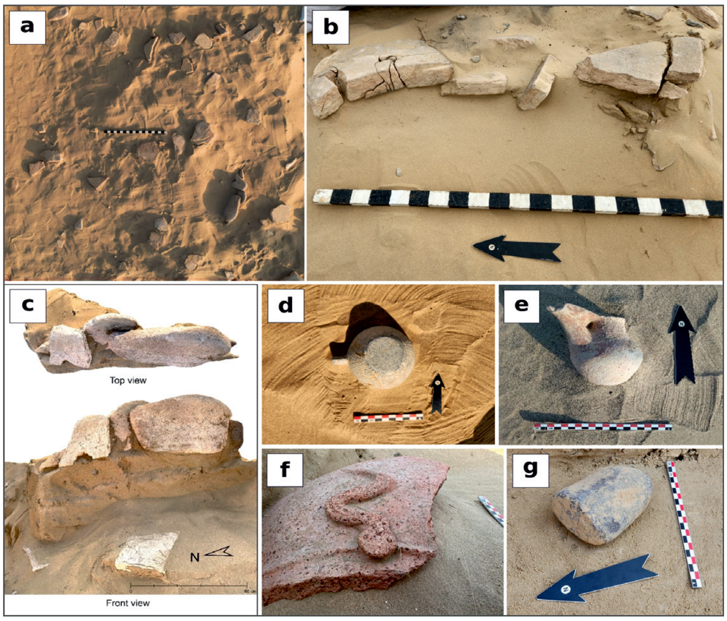

Figure 6. *Phase 2. a) Aerial view of Square U11. b) Structure 3. c) Structure 2. d) Complete soft-stone vessel found upside down. e) Complete bridge-spouted vessel. f) Pottery sherd with snake decoration. g) Hammer stone tool associated with metallurgy.*

2.2 Area T, Phase 3

Squares V6 and V7 are located immediately east of the 2018–2019 excavation grid, where a charcoal production area had previously been documented (Boraik 2020). The 2025 intervention exposed four layers. Layer 1, the uppermost deposit, consists of aeolian sand with modern intrusions and contains no archaeological material.

Phase 3 comprises fourteen pits cut into the gypsum bedrock and the overlying dump sequence of Layers 2–4, attributed on radiocarbon grounds to the second half of the Iron Age II. Feature 10 (298 × 229 × 37 cm) (Fig. 7a) is the only feature of sufficient volume for sustained charcoal production under controlled oxygen supply (Mooney 2011; FAO 1985); In addition, squares V6 and V7 contained several smaller pits, and combustion features whose precise function cannot be determined. However, they were probably related to small-scale combustion activities, possibly including occasional food consumption, as suggested by the burnt animal bone recovered from Feature 8 in V7.

No slag or metallurgical residues were recovered from any of them. Context 10, a sandy layer, seals Feature 10, marking the end of its primary use before charcoal deposition resumed in the same area. Layers 2–4 represent successive episodes of charcoal-rich waste dumping (Fig. 7b-8), each separated by thin aeolian sandy lenses indicating brief periods of inactivity. Artefacts embedded in the dump layers include two ceramic bowls left in situ at the top of Layer 4 (Fig. 7c), two metal fragments possibly from a dagger in the same layer, and a small complete jar in Layer 2 (Fig. 7d) alongside two slag fragments; the absence of further metallurgical evidence in primary contexts suggests these slag fragments represent secondary deposition.

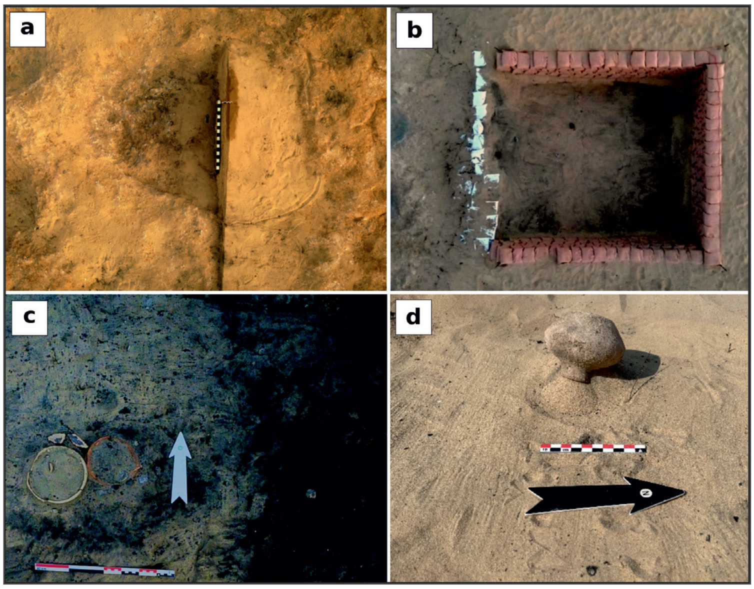

Figure 7. *Phase 3. a) charcoal production pit. b) Aerial view of layer 3 within V6. c) two ceramic bowls left in situ at the top of layer 4 (V7). d) complete small jar found upside down within layer 2 (V6).*

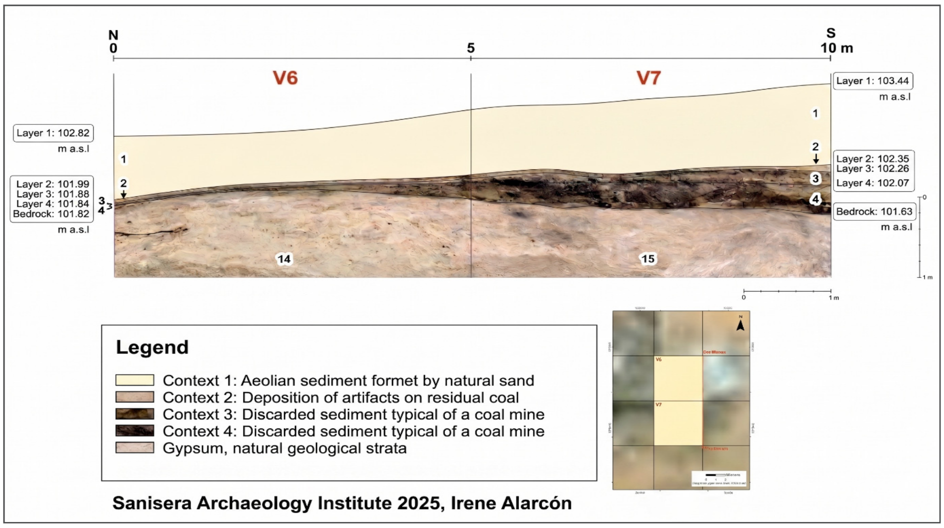

Figure 8. *West facing stratigraphic section of V6 and V7.*

2.3 Radiocarbon Dating

The relative sequences described above for Areas O and T were placed on an absolute timescale through a programme of AMS radiocarbon dating (Table 1). Eleven samples — charcoal and bone bioapatite — were submitted for AMS radiocarbon dating at the FTMC laboratory (Vilnius, Lithuania), using a Low-Energy Accelerator and Automated Graphitization Equipment AGE-3. Bioapatite samples were prepared with sodium chlorite and acetic acid; charcoal samples underwent standard acid–base–acid pretreatment. Calibration used OxCal 4.4 (Bronk Ramsey 2009) and the IntCal20 curve (Reimer et al. 2020), with a Bayesian sequential model incorporating stratigraphic priors and a 5% outlier probability (Fig. 9). The only determination available for Phase 1 — a bioapatite sample from Layer 3 (SH.SAN.355, Square V12, Context 15) — yielded a result inconsistent with its stratigraphic position and was excluded, given the susceptibility of bioapatite to diagenetic alteration. The Bayesian model realized therefore directly dates only Phase 2 and Phase 3; Phase 1, lacking any reliable absolute determination, is placed solely on stratigraphic grounds, below the dated Layer 2.

Phase 2 (Layer 2, Area O) dates to c. 891–772 cal BCE (95.4%), with highest probability density at c. 837–786 cal BCE (68.3%), within the 9th–early 8th century BCE. Phase 3 (Layers 2–4, Area T) dates to c. 776–436 cal BCE (95.4%), with highest probability density at c. 767–654 cal BCE (68.3%), which places it in the second half of the Iron Age II and makes it the most recent activity documented in the campaign.

Table 1. *Radiocarbon determinations from SAR53, 2025 season.*

Sample ID	Lab Code	Material	Area/Square	Context	^{14}C Age (BP)	Cal BC (95.4%)
SH.SAN.361	FTMC-ZN36-13	Cremated bone	O / U11	C3	2707 ± 29	c. 909–807
SH.SAN.360	FTMC-ZN36-12	Charcoal	O / U11	C2	2634 ± 36	c. 898–771
SH.SAN.358	FTMC-ZN36-10	Bone (bioapatite)	O / V13	C2	2670 ± 29	c. 900–794
SH.SAN.359	FTMC-ZN36-11	Bone (bioapatite)	O / V13	C2	2603 ± 30	c. 821–761
SH.SAN.364	FTMC-ZN36-16	Charcoal	T / V6	C13	2455 ± 29	c. 755–415
SH.SAN.366	FTMC-ZN36-18	Charcoal	T / V7	C4	2473 ± 32	c. 769–422
SH.SAN.362	FTMC-ZN36-14	Charcoal	T / V6	C3	2424 ± 34	c. 750–402
SH.SAN.363	FTMC-ZN36-15	Charcoal	T / V7	C3	2451 ± 31	c. 755–412
SH.SAN.365	FTMC-ZN36-17	Charcoal	T / V7	C2	2505 ± 31	c. 780–523

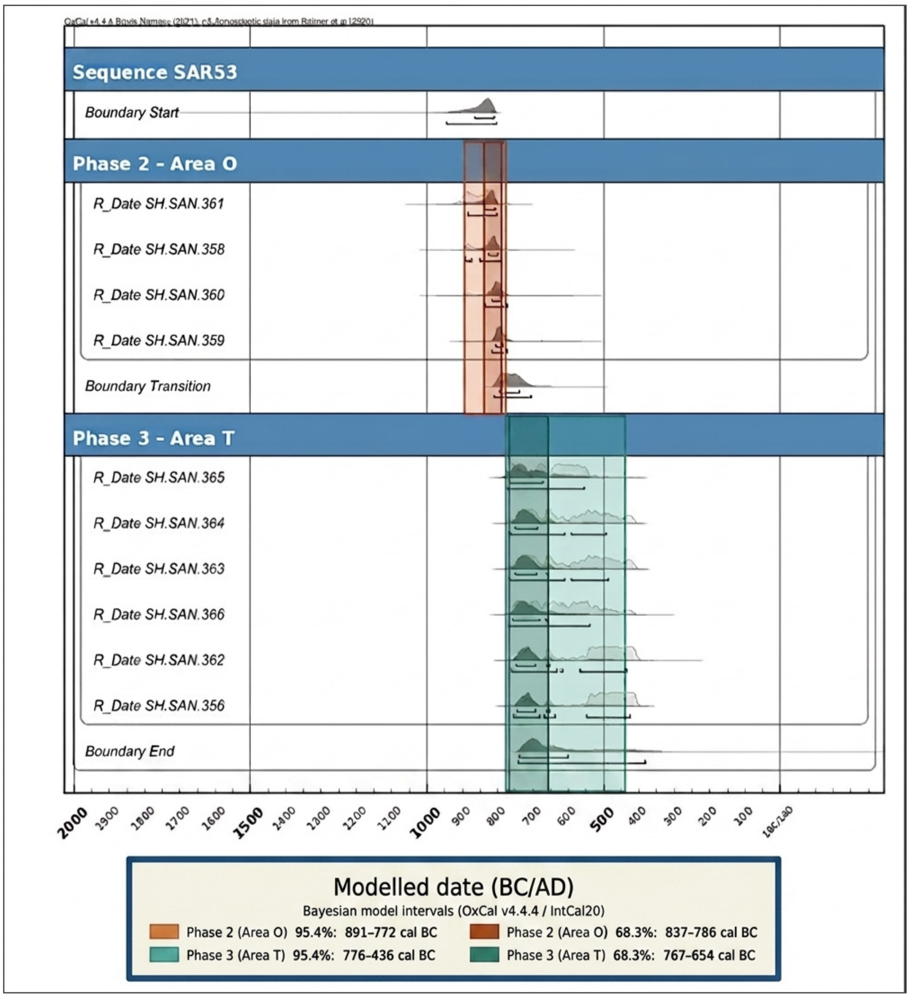

Figure 9. *Bayesian chronological model for SAR53, showing the calibrated radiocarbon dates from Phase 2 in Area O and Phase 3 in Area T. Calibration was performed in OxCal v4.4 (Bronk Ramsey 2009) using the IntCal20 calibration curve (Reimer et al. 2020). Modelled date ranges are expressed in cal BC at 68.3% and 95.4% probability.*

3. Metallurgical Evidence

Metallurgical activity is concentrated in Phase 2 (Area O) and reflects several stages of the copper working. The excavation recovered numerous pieces of metallurgical slag, sorted into two Type 1 and Type 2 (Fig. 10). Slag Type 1 is characterised by a highly vesicular and vitrified structure, while slag Type 2 presents a more granular and less vitrified appearance. Detailed analysis was carried out on a representative piece of each type (Type 1: SH.SAN.303; Type 2: SH.SAN.304). The Type 2 piece is waste that stayed in the furnace during smelting, and it still holds a half-reacted scrap of the original copper ore. This provides clear evidence that copper ore was being smelted on the spot; the faint trace of tin it contains came in naturally with the ore rather than being added on purpose. The Type 1 piece is cleaner, with hardly any metal trapped inside, and seems to have been drained off from the furnace while still molten. Both pieces, and the copper found with them, contain tiny droplets of a copper-and-iron sulphide — exactly what one would expect when the local, sulphur-rich copper ores are smelted.

Figure 10. *Slag Type 1 (left) and slag Type 2 (right) recovered from Layer 2 (Area O).*

Two metallic products, corresponding to two successive stages of copper production, were also distinguished. The first is black copper, produced by primary smelting under highly reducing conditions, with high metallic iron contents (13–27%) and significant cobalt (up to c. 1%). The second is refined copper obtained from it through a subsequent oxidising process that selectively removed the iron, yielding a much purer metal (iron below 3%, cobalt below 0.25%); the refining slag associated with this stage is rich in magnetite rather than fayalite, as expected for a process aimed at iron removal. One refined-copper specimen contains c. 12% tin, identifying it as a bronze residue from a remelting operation and attesting to the reworking of alloys on site.

Ingots show the composition and microstructure of black copper at an intermediate stage of processing, with very high iron levels, confirming that the metal had not yet undergone full refining. The finished objects are of much purer, refined copper, and their trace-element pattern closely matches both the refined copper and a corroded copper prill (SH.SAN.259) from the assemblage. This similarity is consistent with the objects having been made from copper produced at SAR53, although the analysis cannot establish this with certainty.

Alongside the ingots, the assemblage contains scrap metal — broken and deliberately cut copper fragments collected for remelting. The single bronze residue (SH.SAN.316), carrying c. 12% tin in an assemblage otherwise of unalloyed copper, fits this picture: because deliberately alloyed metal cannot result from smelting copper ore, it most likely derives from the remelting of an existing bronze object, though the alloying of fresh copper with tin on site cannot be ruled out.

The presence of selenium detected in chalcocite inclusions across multiple object types is consistent with the well-established model of copper supply from the Oman Peninsula, where Omani ores characteristically contain selenium and tellurium (Prange 2001; Begemann et al. 2010); definitive provenance confirmation would require lead isotope analysis, not yet carried out on this assemblage.

Of particular significance is a copper–silver alloy containing approximately 47% silver and 51% copper, with minor tin (c. 1.2%) and lead (Fig. 11). Its wire-like, elongated morphology and composition — close to the ideal ratio for silver hard solder (c. 60% Ag, 40% Cu) — suggest it functioned as a brazing alloy for joining parts of silver objects. Copper–silver alloys of this kind have not previously been identified at Saruq al-Hadid.

Three stone tools point to metalworking: a grooved hammerstone (13 × 11.1 × 5.4 cm) - the first recorded at Saruq al-Hadid, its hafting groove and heavily worn striking face indicating sustained use — together with a possible second hammerstone and a pointed, edged tool (Fig. 12). They are consistent with hammering and finishing metal, though use in crushing ore cannot be excluded, as at other copper-working sites in the region (Döpper 2020, p. 19). No moulds were recovered, in keeping with their general absence across Saruq al-Hadid. On-site manufacture of finished objects at SAR53 therefore remains an inference — from the abundance of objects, the metal residues, the finishing tools, and the shared trace-element signature linking the locally smelted, pre-refining copper to the refined copper of the finished objects.

The spatial distribution of metallurgical materials is strongly patterned: square U12 yields the highest concentrations of two slag types combined (2,907 g, vs. a maximum of 975 g in V12), while stone tools concentrate in V12 (1,022 g) and V13 (605 g).

Figure 11. *copper-silver object SH.SAN.323 with its elongated part.*

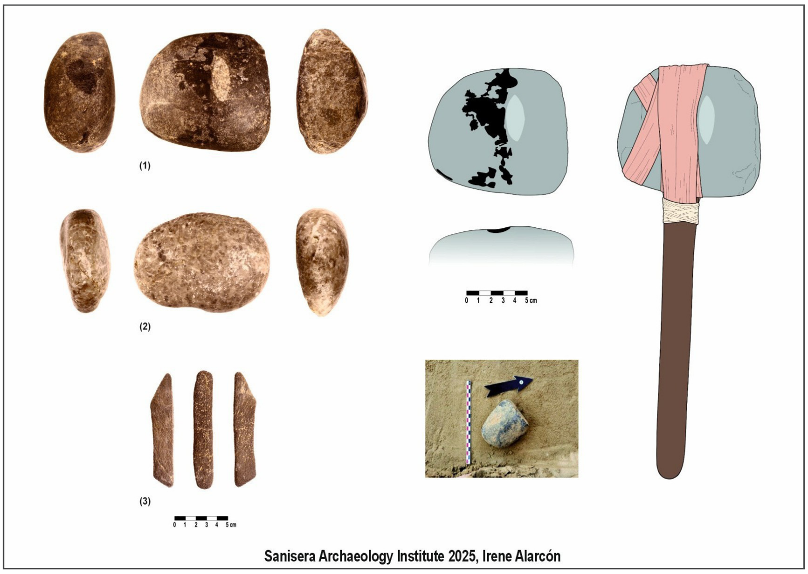

Figure 12. *Stone tools found in Layer 2 (Area O): (1) hammerstone with a possible groove for hafting a handle (represented illustration on the right); (2) possible hammerstone; (3) elongated stone tool with shaped edges and pointed ends*

4. Ritual Assemblage

Layer 2 is strongly characterised by objects whose preservation, composition, and contextual associations suggest deliberate deposition. Several lines of evidence support this interpretation: the predominance of complete or near-complete items over fragmented material; the presence of categories — copper snake figurines, serpent-decorated pottery, jewellery, weaponry, and pigment shells — with no evident functional relationship beyond their symbolic associations; and the recurrence of comparable assemblage compositions at Saruq al-Hadid and other Iron Age II sites in the region (Contreras et al. 2017; Valente 2020; Al Suwaidi et al. 2025; Weeks et al. 2022). Although recovered at varying elevations, likely due to the sloping depositional surface, these materials are interpreted as belonging to a single event or to a closely spaced series of depositional episodes.

Two copper snake figurines were recovered, rendered in elongated sinuous forms with slight head differentiation (Fig. 13a). Their co-occurrence with serpent-decorated pottery (see Chapter 6 for full ceramic description) is a pattern well established at Saruq al-Hadid and comparable regional sites. Soft-stone objects include a complete spouted vessel with geometric incised decoration, several decorated fragments, and small elongated worked elements (Fig. 13b). Jewellery comprises a gold ribbon, metal beads (including plausible lead–silver and lead–gold alloys), carnelian and other small beads, copper rings, a shell bead, and four groups of mixed-material beads possibly corresponding to bracelets or necklaces (Fig.

13c), flat copper elements possibly functioning as spatulas or razors (Fig. 13d). Shells bearing pigment traces were found in association with a copper borer carrying pigment residues (Fig. 13e) and fishhooks (Fig. 13f) The weaponry component includes copper arrowheads of varied morphologies (Fig. 14a) - including miniature double-pointed examples — iron dagger fragments (specimen SH.SAN.82 the most complete) (Fig. 14b). Furthermore, a copper piece interpreted as a possible miniature shield with attached handle (SH.SAN.133) (Fig. 14c).

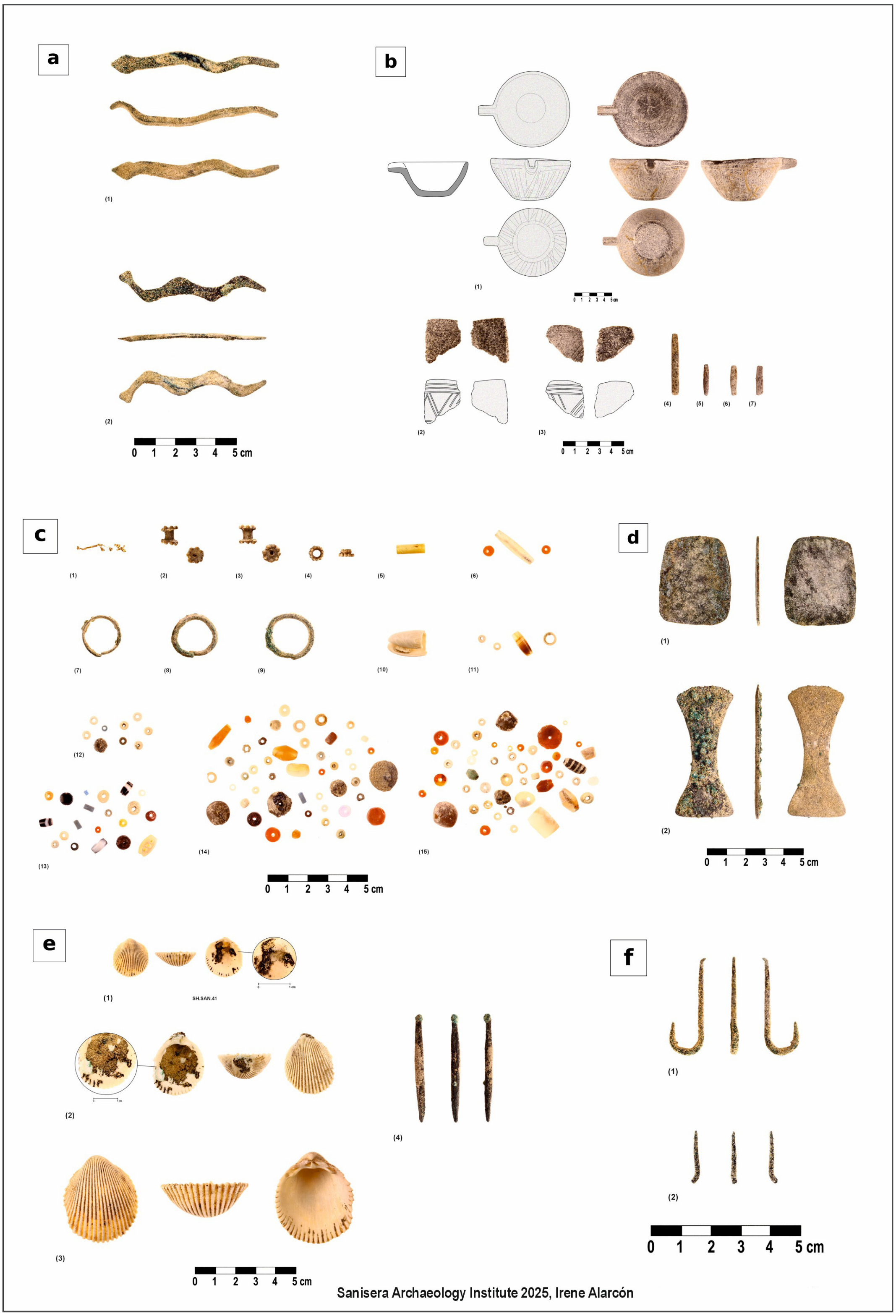

Figure 13. *a) Copper snakes. b) (1) soft-stone spouted vessel with incised decoration; (2–3) soft-stone fragments with incised decoration; (4–7) small elongated soft-stone elements, possibly tools or worked fragments. c) Jewelry). (1) gold ribbon; (2–4) metal beads (5–6, 11) tubular and small beads (light-coloured materials, including carnelian); (7–9) copper rings; (10) shell bead; (12–15) groups of beads (mixed materials), possibly from bracelets and necklaces.d) Copper spatulas. e) (1–3) shells with pigment; (4) borer used for pigment application. f) fishhooks.*

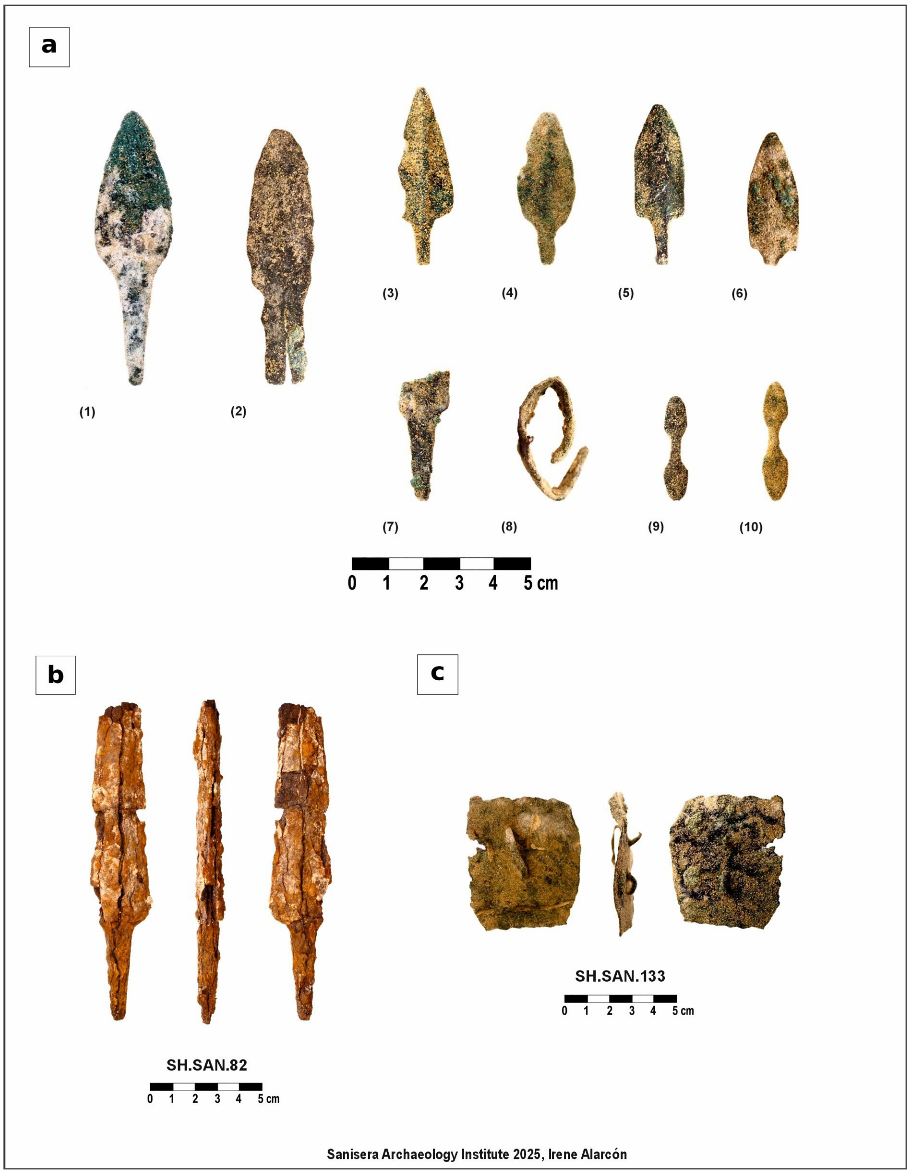

Figure 14. *a) Copper-alloy arrowheads; (8) bent example; (9–10) miniature double-pointed examples. b) Iron dagger. c) Possible miniature of a shield with an attached handle.*

5. Pottery

5.1 Phase 1 (Area O, Layer 3)

The ceramic record of Phase 1 is extremely limited: 7 fragments, no rim sherds, all non-diagnostic coarse utilitarian wares with reddish fabric. The absence of any diagnostic Iron Age II ceramic types confirms the stratigraphic priority of this horizon.

5.2 Phase 2 (Area O, Layer 2)

Phase 2 contains 418 pottery fragments (79.2% of all sherds recovered in the campaign) and 199 rim sherds (88.4% of all rims). The distribution is strongly concentrated: U12 yields 2,217.6 g (34.1% of Phase 2 fragments by weight) and U11 yields 1,839.6 g (15.4%), followed by V12 (1,196.1 g), U13 (793 g), and V13 (252.7 g).

The diagnostic pottery sample analysed in detail comprises twelve vessels. Within this sample, sandy buff wares predominate. These are characterised by a light buff to orange matrix, fine to medium inclusions, and red or orange slips, and are consistent with regional production traditions from the foothill zones of eastern Arabia, with parallels at the Hili-17 workshop in the Al Ain region (Benoist et al. 1998; Benoist & Valente 2017, unpublished report). Common red wares, which show greater fabric variability, may reflect multiple production centres and broader patterns of regional circulation. The most distinctive items include a complete spouted bridge vessel (SH.SAN.51) (Fig. 15a) and vessels bearing snake appliqué decoration (Fig. 16): a bowl with perforated lug (SH.SAN.90–97) with an ascending snake on the upper body (Fig. 16a); a bowl with a handle decorated with appliqué and impressed snake motifs (SH.SAN.87–156) (Fig. 16b); a lid (SH.SAN.38–109–110–127) with a snake following the curved outer perimeter (Fig. 16c).

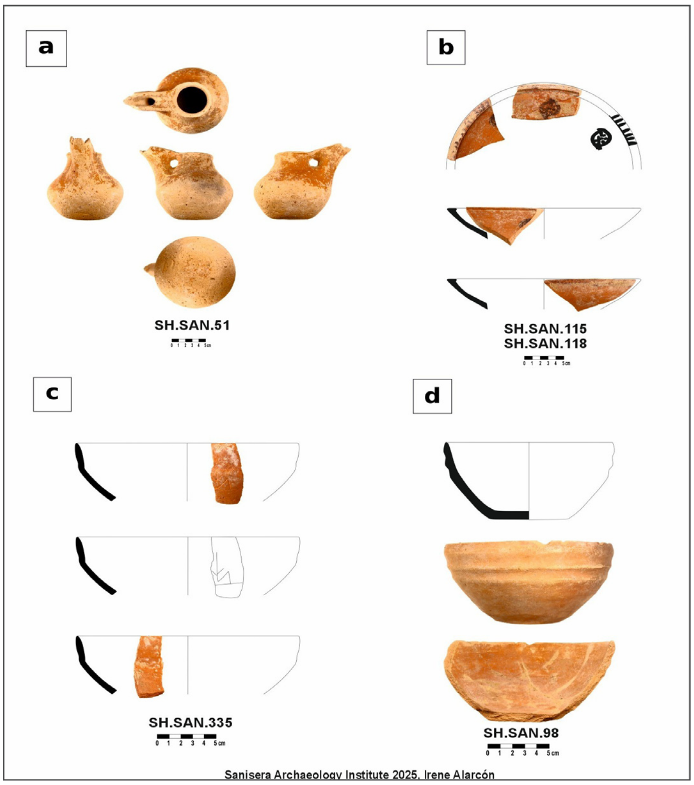

Figure 15. *a) Bridge spouted vessel. b) Bowl with painted geometric motifs. c) Bowl with incised decoration (geometric motif). d) Sandy buff bowl with red to orange slip.*

Additional diagnostic pieces include a painted semi-closed vessel (SH.SAN.30) with geometric zig-zag decoration, a necked jar (SH.SAN.119), a carinated bowl with incised geometric motifs (SH.SAN.335), and two painted bowls (SH.SAN.75; SH.SAN.115–118). Snake motifs are executed as appliqué elements added prior to firing, occasionally further modified by impressed circular marks evoking scales — a technique consistent with comparable assemblages from Saruq al-Hadid and neighbouring sites (Karacic et al. 2017; Benoist & Valente 2017). This ceramic type is documented across Iron Age II UAE and Oman, consistently linked to cult-related activities and appearing in conjunction with copper objects at Saruq al-Hadid (Benoist 2008; Karacic et al. 2017).

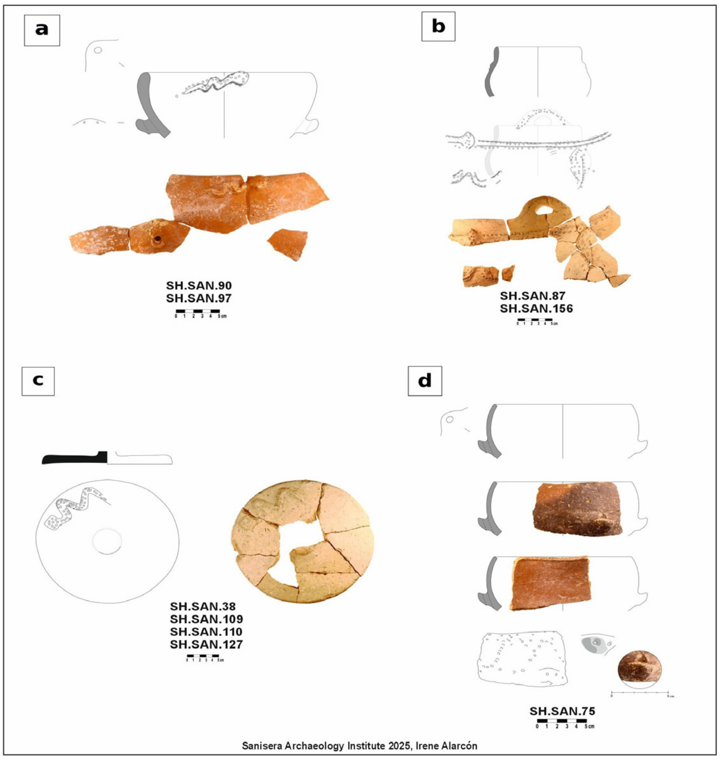

Figure 16. *a) Snake-decorated bowl with perforated lug. b) Bowl with a handle attached to the rim, decorated with snake motifs. c) Snake-decorated lid. d) Bowl with a perforated lug and snake decoration. © Irene Alarcón*

5.3 Phase 3 (Area T)

Area T yielded 103 pottery fragments and 25 rim sherds, distributed primarily in V7 (88 fragments, 15 rim sherds) and V6 (15 fragments, 10 rim sherds). All are attributable to the Iron Age II but lack the diagnostic snake-appliqué decoration characteristic of the Phase 2. The single complete diagnostic vessel is a small hole-mouth jar (SH.SAN.33, sandy buff ware with traces of linear painted decoration), recovered alongside two slag fragments in Layer 2 of V6.

6. Fauna

The faunal assemblage from SAR53 totals 3,609 identifiable remains (NISP): mammals (3,092), fishes (355), birds (3), reptiles (1), marine molluscs (132), and crustaceans (26). Unidentifiable remains constitute 71.04% of the total weight. The assemblage is highly fragmented: 78.65% of remains are smaller than 3 cm, with only 6.34% complete. Taphonomic analysis employed SEM microscopy (Digital Microscope MS100 and TOMLOV TM4K AF, 10 to 2000× magnification) for cut mark characterisation and bone breakage analysis.

6.1 Phase 1 (Area O, Layer 3)

The faunal assemblage from this phase is limited in scale and diversity (NISP = 142). Caprines — combining Ovis aries, Capra hircus, and Caprinae indet. — account for approximately 90% of identified remains; bovids, camelids, and scarce marine resources (isolated fish remains and molluscs) constitute the remainder. A minimum of 18 mammalian individuals are represented, predominantly adults. Very young individuals include an infant caprine under one year (unfused first phalanges) and a prenatal individual represented by a metapodial shaft with gestational division. Thermoalteration is dominated by low-intensity burning: Grade 1 reaches 77.06% of burnt remains (superficial scorching), and Grade 2 (brown-and-black double coloration, diagnostic of roasting in the presence of soft tissues) contributes 9.17%. Advanced grades (4–6) are minor and combined account for c. 10% of burnt remains. The absence of cut marks and intentional bone fracturing, combined with the restricted assemblage size and low taxonomic diversity, supports an interpretation of brief, episodic activity — short-duration cooking associated with the fireplace features rather than sustained occupation.

6.2 Phase 2 (Area O, Layer 2)

Phase 2 concentrates 82.32% of all faunal remains (NISP = 1,099) and shows the greatest taxonomic and anatomical diversity of the campaign. The mammalian assemblage is dominated by caprines (Ovis/Capra NISP = 426; Caprinae indet. NISP = 784), with secondary contributions from Bos taurus (NISP = 23), Camelus dromedarius (NISP = 14), and wild taxa — Gazella arabica (NISP = 8), Oryx sp. (NISP = 6), and Lepus capensis (NISP = 4). All skeletal regions of sheep and goat are represented (MNE = 300), with cranial elements (primarily teeth) and forelimb elements most abundant and axial elements least represented. The total MNI across all taxa is 54 individuals: sheep and goats (MNI = 36 combining Capra/Ovis and Caprinae), camelids (5), gazelles (2), cape hare (2), cattle (1), and oryx (1).

Age profiles indicate a clear predominance of young individuals: infants and juveniles account for 57.57% of identified caprines, and 100% of identified cattle and gazelle individuals are immature. Detailed age estimates include a neonate under 15 days (unerupted dp4), two individuals under 1 month, three under 3 months, and six under 1 year, followed by five juveniles between 1 and 2.5 years and one between 2.5 and 3 years. A juvenile camel between 2 and 3.5 years, a cattle individual with its first molar in the final stages of eruption (under 1 year), and two gazelles slaughtered in their first year of life complete the picture. This demographic structure — a continuous sequence from neonates to young adults — points unambiguously to a meat-oriented exploitation strategy centred on young animals, consistent with structured communal consumption.

Taphonomic evidence confirms intensive anthropogenic processing. Cut marks are documented on caprines and small mammals: a disarticulation mark on the distal epiphysis of a left ovine humerus; an oblique incision on a sheep/goat scapula neck (disarticulation); defleshing marks on ribs; extraction-of-viscera marks on rib ventral surfaces; dismemberment marks on vertebral apophyses; and defleshing marks on long bone shafts. Long bone fractures document systematic marrow extraction: 88 bones with clear green fractures (84.09% from this phase), all on limb bones of sheep, goats, and camels, accompanied by 25 bone flakes produced by fracturing fresh bone.

Marine resources are strongly represented, providing evidence of regular connections between the coast and the desert interior. Fish constitute the second most abundant vertebrate group (n = 355 remains, 78.87% from this context), concentrated in U12-C2 (29.01%), U12-C4 (17.75%), and V12-C2 (11.83%). Vertebrae of Carcharhinus sp. in anatomical connection confirms the transport of sharks (requiem sharks, Carcharhinus sp.) to the site (Fig. 17a); remains of Carangidae and Chanos chanos, characteristic of coastal waters, complement the picture of provisioning from shallow coastal environments. Marine molluscs (n = 132) combine edible bivalves — Rugalucina angela (31.11% of bivalves), Dosinia alta (17.78%), Notocallista umbonella and Vasticardium lacunosum (11.11% each) — with ornamental forms including intentionally perforated specimens: a Nerita polita with a regular circular perforation at the apex, and a Barbatia ublicuata with a complete circular perforation consistent with suspension by cordage (Fig. 17b). All 26 crustacean remains, exclusively barnacles (family Balanidae), derive from this context; as sessile organisms attached to hard marine substrates, they were most likely transported already attached to shells or other materials.

Thermoalteration in Phase 2 shows the broadest spectrum and highest thermal intensities of the campaign. Grade 4 (black-and-white colouring, less than half charred) predominates at 40.59% of burnt remains; Grades 5 and 6 combined exceed 21%, indicating temperatures above c. 800°C in a substantial portion of the assemblage (Nicholson 1993), consistent with proximity to the possible metallurgical combustion features in U11–U12. Grade 2, reflecting roasting in the presence of soft tissues, reaches 12.35%, documenting culinary processing within the same spatial zone. This combination of high-grade calcination and roasting documents a heterogeneous thermal regime in which food preparation and high-temperature metallurgical or fire-cleaning events coexisted.

The spatial distribution of faunal remains is clearly structured. By total weight, V13 accounts for 51% of the phase 2 assemblage (c. 6,058 g), while burnt bones peak in U11 (49.5 g) and U12 (37.6 g). The integration of this pattern with the distribution of the other material classes is presented in Section 8.

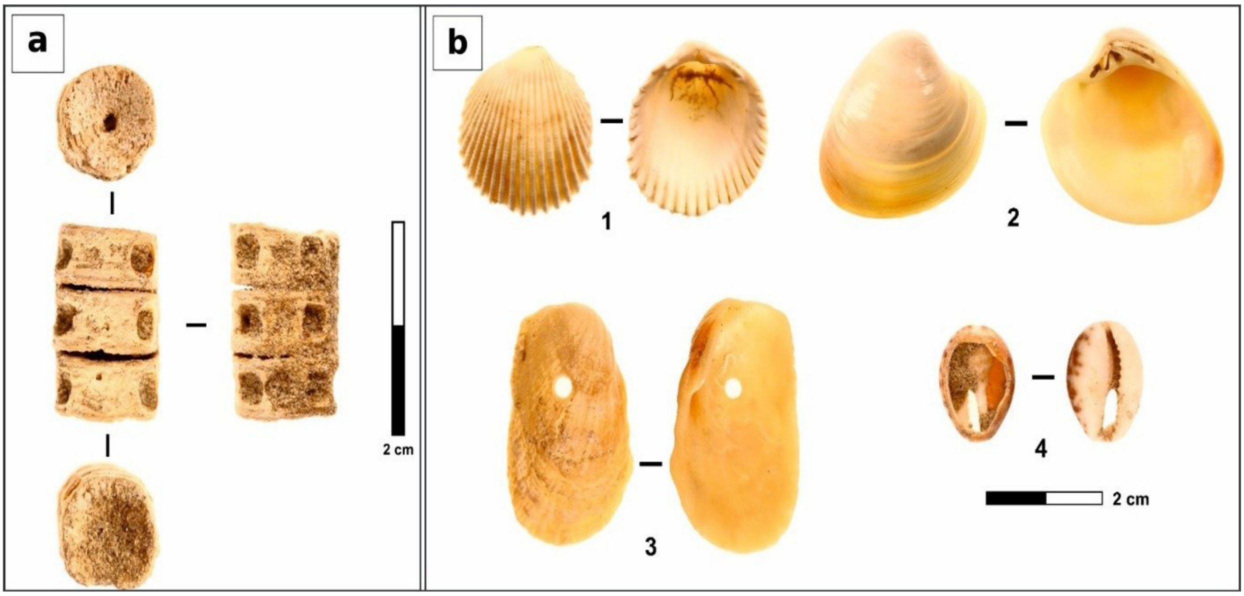

Figure 17. *a) Vertebrae of Carcharhinus sp. in anatomical connection. Phase 2, Area O. b) Shells recovered, Phase 2, Area O. 1) Vasticardium lacunosum. 2) Notocallista Umbonella. 3) Perforated Barbatia ublicuata. 4) Cypraea tigris.*

6.3 Phase 3 (Area T)

The Phase 3 faunal assemblage is limited (NISP = 54) and consists exclusively of mammalian remains with marked caprine dominance (64.81%). Cattle and camelids are marginally represented; no wild taxa are present; no marine resources were recovered. A minimum of 12 individuals are identified, primarily sheep and goats. The age profile includes an infant caprine under one year (unfused first phalanges), an infant camel under one year (unerupted molar), and a prenatal caprine represented by a metapodial shaft with gestational division. Thermoalteration is dominated by low-intensity burning (Grade 1 = 77.06%), with Grade 2 at 9.17% indicating roasting; higher grades are minor. No cut marks or intentional bone fracturing were documented. The overall pattern reflects low-intensity, localised activity centred on caprine consumption and routine roasting, with no evidence of marine resource exploitation or high-temperature burning, distinguishing it from the larger, more diverse and more thermally varied Phase 2 assemblage.

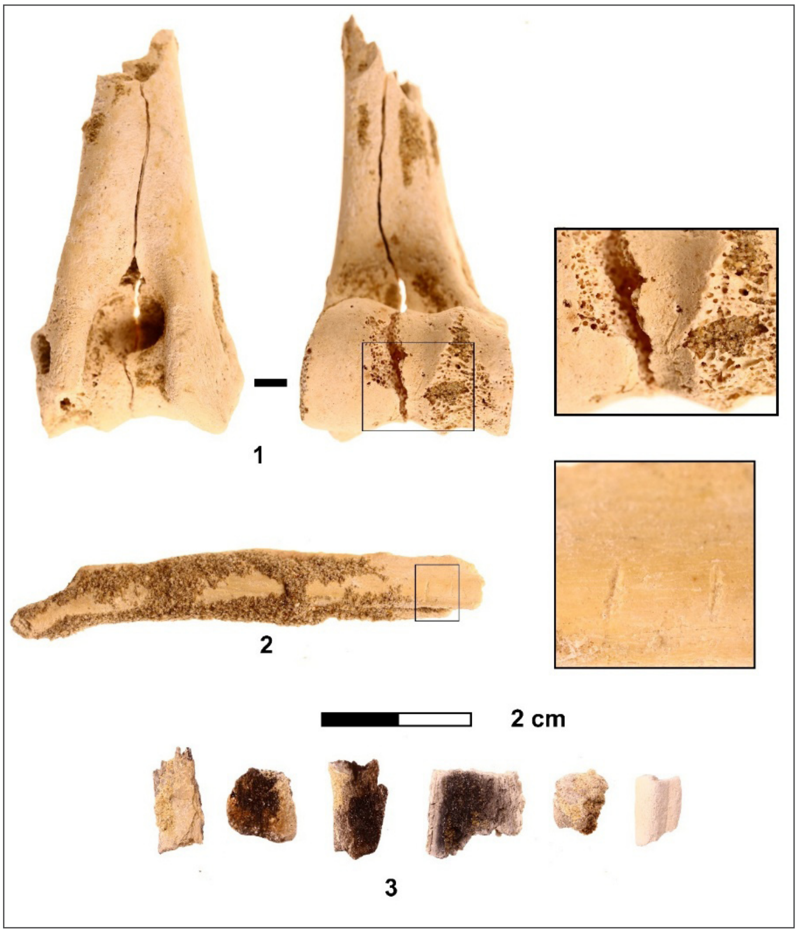

Figure 18. *Anthropogenic modifications on the faunal remains from Saruq Al Hadid. 1) Humerus of Ovis aries with a disarticulation cut mark. 2) Vertebral apophysis with dismemberment cut marks. 3) Different burning colourations left to right, grades 1 to 6.*

7. Anthracology

Anthracological analysis was conducted on 237 charcoal fragments. The flotation samples provided important methodological information, demonstrating that water immersion is unsuitable for the recovery of taxonomically informative charcoal in this context. The charcoal, affected by hygroscopic salts, underwent severe fragmentation during flotation and could only be identified as indeterminate dicotyledonous angiosperms. This outcome is consistent with previous observations from saline desert sites, where salt-bearing charcoal is particularly vulnerable to disintegration during water-based recovery procedures (Arranz-Otaegui 2017; Weeks et al. 2017).

7.1 Phase 2 (Area O, Layer 2)

Analysis of hand-recovered samples identified seven woody taxa: Acacia tortilis type, Chenopodiaceae, Ficus cf. sycomorus, Moringa sp., Nerium oleander, Pistacia sp., and Tamarix sp. Ficus cf. sycomorus and Tamarix sp. were the most ubiquitous, suggesting either preferential selection for fuel or greater availability in the immediate environment. Small-diameter wood with a large number of branches is particularly well represented, consistent with opportunistic collection of available scrub.

The assemblage is entirely consistent with locally procured, drought-adapted taxa characteristic of the Euphorbia larica–Acacia tortilis vegetation zone of the Arabian Peninsula. Notably, the presence of water-dependent taxa — Nerium oleander, Ficus cf. sycomorus, and Pistacia sp. — implies that the immediate surroundings of SAR53 during Iron Age II supported more mesic microhabitats than today, likely associated with ephemeral watercourses or oasis margins now disappeared. This inference aligns with broader palaeoenvironmental evidence for progressive vegetation decline in southeastern Arabia between the fourth millennium BCE and the first millennium CE (Roberts et al. 2020) and finds close parallels in the Acacia–Tamarix–Chenopodiaceae woodland assemblages documented at Bronze Age sites in Oman (Deckers et al. 2019) and the Iron Age site of Salut (Bellini et al. 2011). The exclusively local character of the SAR53 charcoal indicates that the woodland of the immediate surroundings was sufficient to meet the site's fuel needs, without recourse to wood brought from further afield. No worked wood objects of the kind reported at sector SAR7, made on non-local taxa such as Olea europaea, Pinus sp. and Rhizophoraceae, were recovered at SAR53 (Weeks et al. 2017, p. 39).

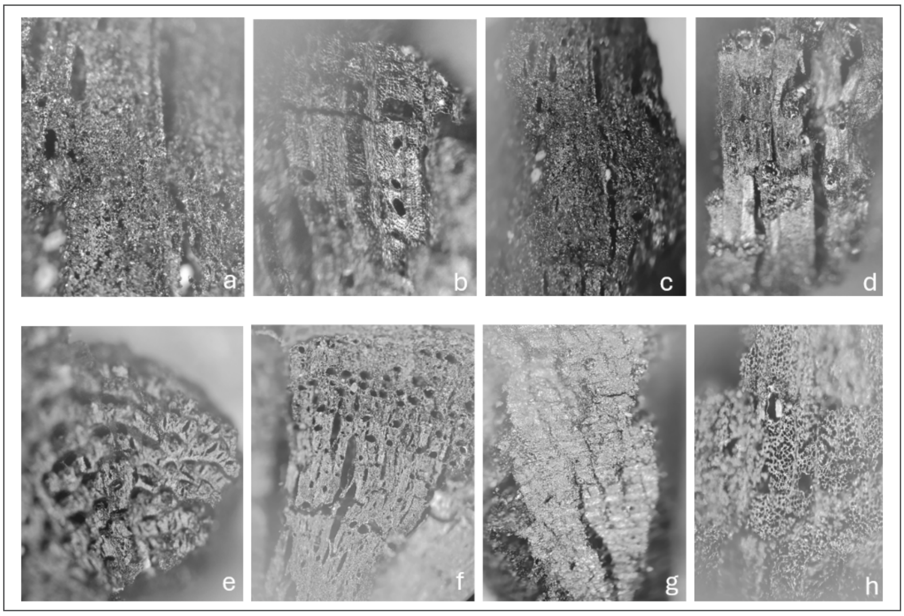

Figure 19. *Transverse section for angiosperm dicotyledonean undeterminable (a), Tamarix sp. (b), Nerium oleander (c), Ficus cf. sycomorus (d), Chenopodiaceae (e), Pistacia sp. (f), Acacia cf. tortilis (g), Moringa sp. (h), 40x magnification metalographic microscope dark field.*

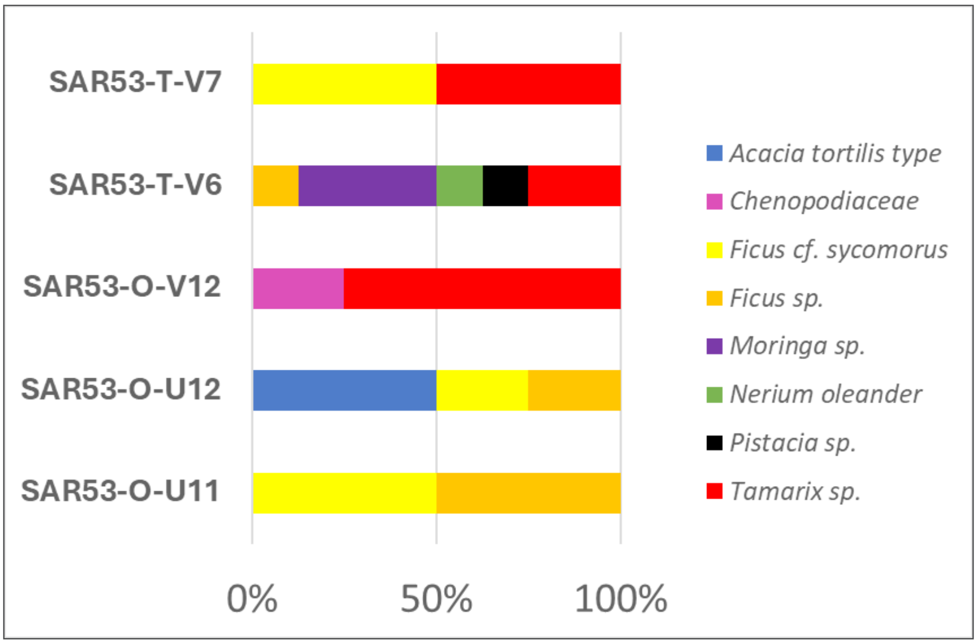

Figure 20. *Anthracology taxa chart for SAR53.*

7.2 Phase 3 (Area T)

The charcoal assemblage from Phase 3 identifies the same broad suite of locally available taxa as Phase 2: Nerium oleander and Ficus cf. sycomorus are the most precisely identified species, alongside Acacia sp., Moringa sp., Pistacia sp., Tamarix sp., and a proportion of indeterminate dicotyledonous angiosperms. The functional context — dedicated to charcoal production and systematic waste disposal — suggests that the taxa here reflect sustained and organised fuel procurement oriented towards supplying metallurgical operations across the site. The persistence of water-associated taxa into Phase 3 reinforces the interpretation of a locally more mesic microenvironment toward the end of Iron Age II.

8. Spatial Organisation (Phase 2, Area O)

GIS analysis of Phase 2 material distributions reveals a structured, non-random organisation of activities within Area O. Directional ellipses for all ritual material categories — pottery, soft-stone objects, jewellery, weapons, pigment shells, copper snake figurines, spatulas, and fishhooks — show clear convergence on square U12. The cumulative raster surface, constructed by summing unit-value rasters derived from each category ellipse, consistently identifies U12 and its immediate surroundings as the zone of maximum spatial convergence, interpreted as the central focus of ritual activity.

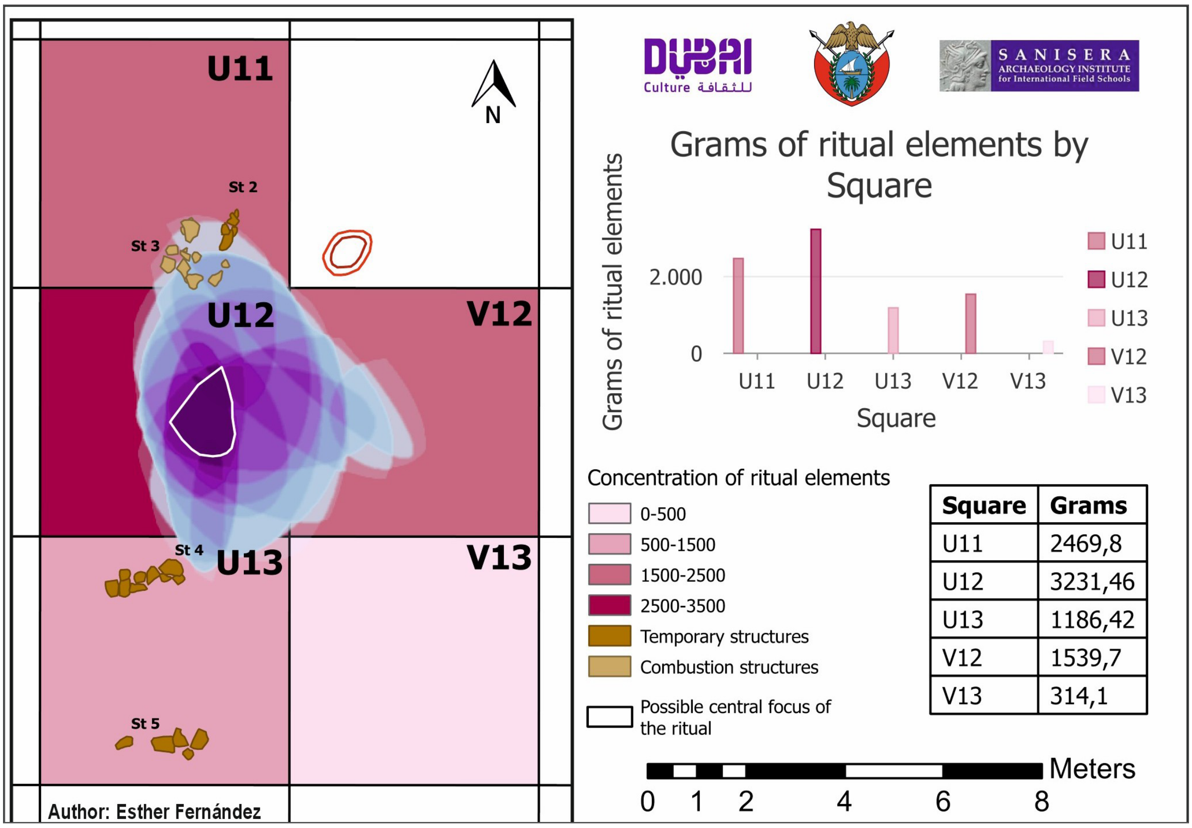

Figure 21. *Grams of ritual elements by square and central focus of the ritual in Phase 2.*

The distributions of the individual material classes, reported in the preceding sections, converge on the same spatial structure. Slag and the full ritual assemblage — serpent-decorated pottery, copper figurines, soft-stone objects, weaponry, jewellery and pigment shells — share their maximum density in U12, identifying this square as a combined production-and-deposition core, with a slight projection of metallurgical debris toward U11. The bulk of the pottery follows the same pattern, peaking in the U11–U12 axis. Against this core, stone tools and the principal faunal accumulation diverge: their directional ellipses are oriented along a north–south axis toward a V12–V13 periphery, spatially detached from the metallurgical-ritual focus. This consistent partition between a U12 core and a southern periphery is one of the clearest functional differentiations in the Phase 2 assemblage.

The faunal evidence sharpens the same picture. Burnt bone peaks in the U11–U12 sector, coinciding with the combustion features inferred for that area, and falls away sharply to the south (U13, 1.7 g; V13, 2.6 g). Total faunal weight, by contrast, concentrates overwhelmingly in V13 — a square detached from the metallurgical-ritual core and consistent with a discard zone for consumed animals. Formal spatial-statistical analysis of the burnt-bone distribution (Getis-Ord Gi*, Global Moran's I [$I = 0.37$, $p \approx 0.09$], Anselin Local Moran's I [$R^2 \approx 0.77$]) indicates an incipient but non-random organisation at the local scale, with high-value cells tending to cluster, supporting a distribution conditioned by defined activity zones rather than random deposition.

Taken together, these independent lines of evidence describe a single, internally ordered space: ritual deposition and metalworking converging in U12, food preparation and combustion-related activity in the U11–U12 sector, and the discard of consumed fauna held at a distance in V13. Because each material class was recovered and analysed separately, their convergence on the same arrangement provides mutually reinforcing support for a deliberately structured use of space rather than an artefact of any single dataset. The cumulative GIS probability surface, derived from the geometric coherence of these distributions and the orientation of their main dispersion axes, identifies squares T11, T12 and T13 as the areas of highest potential for future campaigns.

9. Discussion

The stratigraphic and material evidence from Areas O and T defines three phases of activity at SAR53, each with a distinct functional signature. Phase 1 (Layer 3, Area O) represents the earliest documented use: low-intensity, episodic occupation without diagnostic Iron Age II material culture. Its significance lies not in its material richness but in establishing prior use of the terrain before the exceptional Phase 2 episode, and in the total contrast it presents with the overlying horizon.

Phase 2 (Layer 2, Area O; 9th–early 8th century BCE) is defined by the simultaneous presence of metallurgical production evidence and an extraordinarily rich ritual assemblage concentrated around square U12, pointing to a specific, orchestrated episode or closely related series of events. Phase 3 (Area T; c. 767–654 cal BCE at 68.3 %), chronologically later and spatially distinct, reflects systematic charcoal production and management — a logistical prerequisite for the metalworking operations evidenced in Phase 2 and across the broader SAR53 landscape.

The co-occurrence of metallurgical and ritual material in Phase 2 is the central interpretative question raised by the 2025 data, and it is worth being precise about what the archaeometallurgy demonstrates and what it allows us to infer. Two stages of the operating sequence are securely demonstrated on site (Section 3): primary smelting — attested by furnace slag that still encloses a partially reacted relic of the original ore, direct proof of reduction on the spot — and refining, recorded in the transition from iron-rich black copper to a much purer refined product. A copper–silver alloy close to the composition of silver hard solder further adds specialised joining techniques not previously documented at Saruq al-Hadid.

The manufacture of the finished objects themselves on site is, by contrast, an inference rather than an established fact. It rests on the close trace-element match between the refined copper, a corroded copper prill, and the finished artefacts, together with the hammerstones and finishing tools present in the assemblage; but no moulds were recovered — in keeping with their general absence across Saruq al-Hadid — What the deposit captures most clearly is not an isolated metallurgical episode, but a broad segment of the copper chaîne opératoire condensed into a single layer: smelting and refining slags, black copper, ingots, scrap collected for remelting, a tin-bearing bronze remelt residue, refined copper, and finished objects, placed together with copper snake figurines, serpent-decorated pottery, and jewellery in square U12. On this reading the 'ritual economy' model proposed for Saruq al-Hadid (Weeks et al. 2022), in which metallurgical craft and ceremonial deposition are mutually constitutive rather than separate spheres of practice, applies directly to Phase 2.

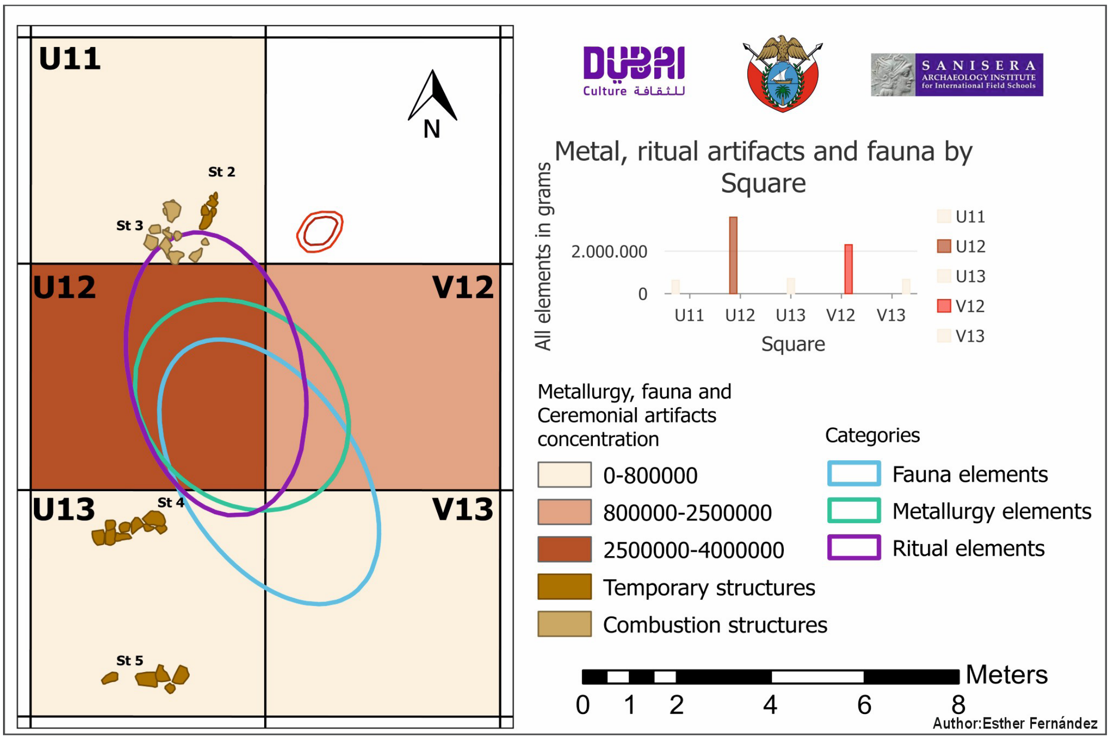

Figure 22. *Spatial distribution of metallurgy, ritual and fauna elements in Phase 2.*

The faunal evidence adds a dimension of communal consumption integral to the broader event. Burnt bone concentrates in the U11–U12 sector, where thermoalteration ranges from roasting-grade scorching to calcination, indicating exposure to both moderate cooking temperatures and higher-energy burning episodes. The features responsible for this burning cannot yet be characterised: in U11, Structure 3 — a tightly arranged stone cluster curving around Structure 2 and recovered some 0.7 m below it — could not be excavated, and its possible function as a combustion feature is inferred only from the charcoal concentrated around it. Because excavation in U11, U13 and V13 was halted at Layer 2 when these stone structures appeared, it remains open whether the adjacent and underlying squares contain installations linked to metalworking or hearths used for food preparation. The spatial contrast between this burnt-bone sector (U11–U12) and the principal discard zone (V13, 51% of the Phase 2 faunal weight) nonetheless points to structured episodes of animal slaughter, preparation, and consumption. The demographic structure of the assemblage — dominated by young caprines, with a continuous sequence from neonates to juveniles — can be an indicative of the slaughter of prime animals for a specific occasion rather than routine subsistence. The presence of marine resources — fish (including *Carcharhinus* sp.), edible molluscs, ornamental perforated shells, and barnacles associated with this phase — indicates contact with the coast and the transport of resources from beyond the immediate landscape.

Taken together, these strands allow a tentative reconstruction of the ceremonial act itself, and not only of its material residue. The recovery of pigment-bearing shells in direct association with a copper borer carrying pigment residues points to the preparation and application of pigment during the event — an action that would otherwise have left little trace. The pairing of pigment and shell is itself a recurrent feature of Iron Age ritual and funerary assemblages in south-eastern Arabia: pigment-bearing shells are documented in several graves of the Al-Qusais necropolis (Contreras et al. 2025) and at sites such as Tell Abraq and Sharm (Thomas & Potts 1996; Masia 2000).

The slab structures exposed in square U13 (Structures 4 and 5), interpreted as temporary installations, may belong to the same setting: their configuration is consistent with low supports on which objects dedicated to the ceremony, or food consumed during it, could have been placed. On this reading, Phase 2 records not merely a deposit but a staged occasion — pigment prepared and applied, prime animals slaughtered and consumed, and metallurgical and symbolic objects assembled and laid down together — of which the surviving features and finds are the partial, durable remainder.

The evidence from Area T provides a functional complement to the ritual-metallurgical picture of Area O. The combination of a large charcoal production pit (Feature 10), successive dump layers, systematic locally procured fuel taxa, and complete absence of metallurgical residues in the primary combustion features leaves little ambiguity about the primary function of this zone. Area T was dedicated to producing and managing the charcoal that the high-temperature copper operations at SAR53 — and possibly at SAR7 — required. The later chronological position of Phase 3 relative to Phase 2 raises the question of whether fuel production was contemporaneous with the ritual-metallurgical episodes or represents a later, more purely industrial phase; the current radiocarbon resolution does not resolve this definitively. The anthracological evidence reinforces the complementarity between the two areas: the same locally procured, least-effort fuel suite characterises both phases, while the persistence of water-dependent taxa into Phase 3 suggests a shared palaeoenvironmental context of relatively moister conditions than today.

The 2025 results confirm SAR53 as a significant and internally differentiated locus within the Iron Age II site complex of Saruq al-Hadid. The Phase 2 metallurgical assemblage shows strong parallels with the evidence from Areas 2A, F, and G of SAR7 (Valente 2020; Weeks et al. 2022), confirming that multiple stages of the metallurgical chaîne opératoire operated within SAR53 itself. The combination of metallurgical and ritual evidence at SAR53 mirrors the pattern already documented at SAR7: the same functional embedding of craft production within a ceremonial framework appears at multiple discrete loci, suggesting this organisation was a structuring principle of the Saruq al-Hadid landscape as a whole rather than a localised anomaly. GIS modelling shows that the Phase 2 deposit extends westward toward squares T11–T14, which represent the most promising targets for future fieldwork.

10. Conclusion

The 2025 excavation season at SAR53 has substantially advanced understanding of this sector within the Iron Age II landscape of Saruq al-Hadid. Three principal conclusions follow.

First, the stratigraphic and radiocarbon evidence defines three phases of activity, each with a distinct functional signature. Phase 1 documents low-intensity, episodic occupation without diagnostic Iron Age II material. Phase 2, c. 891–772 cal BCE (95.4%) and c. 837–786 cal BCE (68.3%), is defined by the co-occurrence of metallurgical processes with a spatially structured deposit of ritual objects. GIS analysis demonstrates non-random organisation around a focal area in square U12, with food preparation and faunal discard zones spatially differentiated from the ritual-metallurgical core. Phase 3, c. 776–436 cal BCE (95.4%) and c. 767–654 cal BCE (68.3%), documents organised charcoal production in Area T, likely supplying metallurgical operations at SAR53 and SAR7.

Second, the Phase 2 evidence shows that metallurgical activity, ritual deposition, and animal consumption were spatially and functionally integrated within the same depositional episode or closely related series of events. This interpretation is supported independently by the archaeometallurgical evidence, the distribution of ritual objects, the spatial patterning of the faunal assemblage, and the GIS modelling of the deposit. SAR53 therefore provides a new, well-contextualised example of the ritual economy of Saruq al-Hadid, in which metallurgy was embedded within broader ceremonial and social practices.

Third, GIS modelling shows that the Phase 2 deposit extends beyond the current excavation limits toward squares T11–T14. Future targeted excavation of these areas holds the highest probability of recovering additional evidence and clarifying the full spatial extent of this exceptional horizon.

These results mark a point of departure for future campaigns. Continued excavation of the squares adjacent to the Phase 2 core would establish the true scale of metallurgical production at SAR53 and define the extent of its associated structures, while further radiocarbon determinations would refine the internal chronology and tighten the articulation between the three phases. A further question for future work concerns the scale and intensity of metallurgical production at SAR53 during later stages of the Iron Age II, corresponding to the Phase 3 horizon documented in Area T, where charcoal production is currently the best-attested activity. Further work in this direction would help clarify whether fuel manufacture was the dominant activity at this stage within SAR53, or whether it formed part of a broader metallurgical system whose production areas have not yet been fully exposed. Assessed alongside the previously excavated sectors of Saruq al-Hadid — notably SAR7 and Area 2A — the SAR53 evidence already makes a substantial contribution to understanding the wider organisation of metallurgical production and ritual practice across the site.

Acknowledgements

The authors thank the Dubai Culture and Arts Authority, Dr. Mansour Boraik and Dr. Anjana Reddy for their valuable comments. We are grateful to all members of the 2025 field team and to the specialists who contributed analytical work to this study.

11. References

1. Arranz-Otaegui, A. 2017. Evaluating the impact of water flotation and the state of the wood in archaeological wood charcoal remains. Quaternary International 457: 60–73.
2. Al-Khraysheh, F. & An-Nashef, K. 2007. Dubai: Civilization and progress throughout three thousand years. Dubai. [In Arabic].
3. Al Suwaidi, M.A., Al Ali, B.M. & Lehner, J.W. 2025. An Iron Age artefact hoard at Saruq as-Hadid-53, Dubai, UAE: a preliminary study. Proceedings of the Seminar for Arabian Studies 54: 230–246.
4. Begemann, F., Hauptmann, A., Schmitt-Strecker, S. & Weisgerber, G. 2010. Lead isotope and chemical signature of copper from Oman and its occurrence in Mesopotamia and sites on the Arabian Gulf coast. Arabian Archaeology and Epigraphy 21: 135–169.
5. Bellini, C., Condoluci, C., Giachi, G., Gonnelli, T. & Mariotti Lippi, M. 2011. Interpretative scenarios emerging from plant micro- and macroremains in the Iron Age site of Salut, Sultanate of Oman. Journal of Archaeological Science 38: 2775–2789.
6. Benoist, A. 2008. The Iron Age culture in the United Arab Emirates, between 1100 BC and 250 BC. Bulletin of Archaeology, Kanazawa University 29: 31–41.
7. Benoist, A., Le Carlier, C., Goy, J., Degli Esposti, M., Armbruster, B. & Attalaelmanan, G. 2015. Snake, copper and water in south-eastern Arabian religion during the Iron Age: the Bithnah and Masāfi evidence. British Foundation for the Study of Arabia.
8. Boraik, M. 2020. Civilization and archaeology through thousands of years. [In Arabic].
9. Casana, J., Herrmann, J.T. & Qandil, H.S. 2009. Settlement history in the eastern Rub al-Khali. Arabian Archaeology and Epigraphy 20: 30–45.
10. Contreras, F. et al. 2017. Excavations in Area 2A at Saruq al-Hadid. Proceedings of the Seminar for Arabian Studies 47: 57–63.
11. Contreras, F., Alonso, A., Fernández-Sánchez, A., Al Ali, B.M., Boraik, M., Zein, H. & Al Masfari, M.A. 2025. Proposed Chronology of Burial Activity by Period in the Necropolis of Al-Qusais (Dubai, UAE). *Annals of Archaeology* 7(1): 15–27.
12. Deckers, K., Döpper, S. & Schmidt, C. 2019. Vegetation, land, and wood use at the sites of Bat and Al-Khashbah in Oman. Arabian Archaeology and Epigraphy 30: 1–14.
13. Döpper, S. 2020. Ground stone tools from the copper production site Al-Khashbah, Sultanate of Oman. *Journal of Lithic Studies* 7(3): 1–24.
14. FAO. 1985. Simple technologies for charcoal making. Rome: FAO.
15. Gernez, G. & Jean, M. 2021. Excavations of an Iron Age site near Adam, Central Oman. Pages 149–161 in M. Luciani (ed.), The archaeology of the Arabian Peninsula 2. Vienna: Austrian Academy of Sciences.

16. Herrmann, J.T., Casana, J. & Qandil, H.S. 2012. A sequence of inland desert settlement in the Oman Peninsula. Arabian Archaeology and Epigraphy 23: 50–69.

17. Karacic, S. et al. 2017. Ritual practices and metal deposits at Saruq al-Hadid (Dubai, UAE). Proceedings of the Seminar for Arabian Studies 47: 141–156

18. Lehner, J. W., Buffington, A., Jameson, M., Gidding, A., Russ, H., Hesse, P., Fisher, G., Plekhov, D., Kaiser, T., Bastek-Michalska, J., Voas, M., Lafe, J., Murphy, C., Green, J. T., & others. (2025). Archaeological Excavations at Saruq 53: Final Report (Technical Report No. 25-244). University of Sydney & Chronicle Heritage.

19. Masia, K. 2000. Pigment shells from Sharm. *Arabian Archaeology and Epigraphy* 11(1): 22–23.

20. Mooney, S.D. 2011. The analysis of charcoal in peat and organic sediments. Mires and Peat 7: 1–18.

21. Nicholson, R.A. 1993. A morphological investigation of burnt animal bone and an evaluation of its utility in archaeology. Journal of Archaeological Science 20: 411–428.

22. Prange, M. 2001. 5000 Jahre Kupfer im Oman. Bochum: Verlag des Deutschen Bergbau-Museums.

23. Roberts, J., Weeks, L., Fillios, M., Cable, C., al-Aali, Y.Y., Boraik, M. & Zein, H. 2020. The bird remains from Saruq al-Hadid. Quaternary International 543: 71–76.

24. Sanisera Archaeology Institute. 2025. Final Report on the Archaeological Excavations at SAR 53, Areas T and O. Project supervised by DCAA. Unpublished.

25. Santos-Assunção, S. et al. 2025. Ground-penetrating radar and magnetic survey of Saruq Al-Hadid, UAE. Science of Remote Sensing 12: 100249.

26. Stiner, M.C., Kuhn, S.L., Weiner, S. & Bar-Yosef, O. 1995. Differential burning, recrystallization, and fragmentation of archaeological bone. Journal of Archaeological Science 22: 223–237.

27. Thomas, R. & Potts, D.T. 1996. Atacamite pigment at Tell Abraq in the early Iron Age. *Arabian Archaeology and Epigraphy* 7: 13–16.

28. Valente, T. 2020. Five seasons of excavations in Areas 2A and G of Saruq al-Hadid. Isimu 23: 169–182.

29. Valente, T. 2023. Copper Metallurgy at Saruq al-Hadid, Dubai, UAE. Master's Dissertation.

30. Weeks, L., Cable, C., Franke, K., Newton, C., Karacic, S., Roberts, J., Stepanov, I., David-Cuny, H., Price, D., Bukhash, R., Radwan, M. & Zein, H. 2017. Recent archaeological research at Saruq al-Hadid, Dubai, UAE. Arabian Archaeology and Epigraphy 28: 31–60.

31. Weeks, L., Valente, T., Franke, K., Contreras, F., Boraik, M. & Zein, H. 2022. Iron Age copper production and the 'ritual economy' of Saruq al-Hadid. Pages 239–270 in Advances in UAE Archaeology. Oxford: Archaeopress.

32. Wygnańska, Z., Bagi, O., Rądkowska, J., Zych, I., Rempel, S., Juchniewicz, K. & Boraik, M.R. 2022. Reconstructing a changing landscape of human activities in the Iron Age II at Saruq al-Hadid. Proceedings of the Seminar for Arabian Studies 51: 449–464.